PCCP

First-order and Gradual Phase Transitions of Ethane Confined in MCM-41

Journal:	*Physical Chemistry Chemical Physics*
Manuscript ID	CP-ART-06-2022-002530.R1
Article Type:	Paper
Date Submitted by the Author:	09-Jul-2022

Complete List of Authors:	Yang, Huan; University of Wyoming, Department of Petroleum Engineering Dejam, Morteza; University of Wyoming, Department of Petroleum Engineering Tan, Sugata; Planetary Science Institute; University of Wyoming, Petroleum Engineering Adidharma, Hertanto; University of Wyoming, Department of Petroleum Engineering, Department of Chemical Engineering

First-order and Gradual Phase Transitions of Ethane Confined in MCM-41

Huan Yang,[a] Morteza Dejam,[a*] Sugata P. Tan,[c] Hertanto Adidharma[a,b*]

[a]Department of Petroleum Engineering, College of Engineering and Applied Science, University of Wyoming, 1000 E. University Avenue, Laramie, WY 82071-2000, USA
[b]Department of Chemical Engineering, College of Engineering and Applied Science, University of Wyoming, 1000 E. University Avenue, Laramie, WY 82071-2000, USA
[c]Planetary Science Institute, Tucson, Arizona 85719-2395, USA

Abstract

The first-order phase transition of ethane confined in MCM-41, i.e., capillary condensation, has been measured through an isochoric cooling procedure utilizing differential scanning calorimetry (DSC) under conditions ranging from 206 K and 1.1 bar up to the pore critical point (PCP). The PCP has also been determined using the three-line method developed earlier based on the vanishing heat of phase transition. As in the bulk phase, no first-order phase transition can occur above the critical point, which also implies that vapor can transform into liquid gradually by following a path around the critical point through supercritical region. For the first time, the gradual phase transition is demonstrated with ethane in MCM-41, which is achieved through a multistep process with paths proceeding around PCP without crossing the capillary-condensation curve. The occurrence of gradual phase transition in nanopores, thus the confined supercriticality, is confirmed while our consistent DSC measurements are also well demonstrated.

1. Introduction

The phase behavior of fluids confined in nanopores is important in various areas including catalysis,[1] separation,[2] gas storage,[3,4] and recovery of shale reservoirs.[5] However, the understanding of such phase behavior is still far from complete, such as the condensation/ evaporation and the shift of pore critical point (PCP) due to nanoconfinement effects. For fluids confined in nanopores, first-order phase transitions, e.g., capillary condensation and evaporation, have been investigated extensively in literatures using various experimental methods, such as adsorption-desorption,[6,7] microfluidic-based,[8] calorimetric-based,[9-17] Nuclear Magnetic Resonance (NMR),[18] and Small-Angle Neutron Scattering (SANS).[19] The adsorption-desorption experiment is the most widely used and thus data from such experiments are more widely available. For example, Morishige et al. measured the capillary condensation of nitrogen, argon, oxygen, and carbon dioxide in MCM-41 and SBA-15 using adsorption-desorption experiments.[6,7]

In recent developments in our labs, we have made alternative measurements using DSC on the capillary condensation/evaporation of pure fluids (i.e., carbon dioxide, ethane, and methane) and binary gas mixtures (i.e., 15±0.3% methane/85∓0.3% ethane and 12±0.24% methane/88∓ 0.24% carbon dioxide) confined in SBA-15/MCM-41 with different pore sizes through an isochoric cooling/heating procedure.[9-15] With the measured capillary condensation data, the PCP

* Corresponding authors.
E-mail addresses: mdejam@uwyo.edu (Morteza Dejam) and adidharm@uwyo.edu (Hertanto Adidharma)

of pure fluids (i.e., carbon dioxide, ethane, and methane) confined in SBA-15/MCM-41 has also been determined using the three-line method,[9,14] whereas that of methane/ethane gas mixture confined in SBA-15 has been bracketed.[13] No first-order phase transition, such as capillary condensation, can occur above PCP, which has been verified in our previous work.[13,14]

When a phase boundary (e.g., condensation curve) is crossed, a first-order phase transition occurs at specific temperature and pressure and involves a latent heat, during which the thermodynamic properties, such as specific volume, internal energy, enthalpy, and entropy, change discontinuously. Therefore, in the supercritical region beyond PCP, continuous changes of those properties are expected. In the bulk, supercritical fluids are considered as a homogeneous phase that allows a continuous gradual transition from gas phase to liquid phase.[20] It is the purpose of this work to verify that the concept of supercritical region is also valid in nanosize confinement, by simply testing the gradual phase transition through the supercritical region that has never been done before. The verification is demonstrated for ethane in MCM-41.

For the records, there were only a few works reporting the capillary-condensation data of ethane in nanopores. He and Seaton measured the adsorption-desorption isotherms of ethane in MCM-41, from which the capillary condensation could be derived.[21] However, the measured capillary condensation for ethane by their measurements was limited since their experimental conditions were close to PCP region and showed near-critical state of ethane, i.e., no distinct step on the isotherm during capillary condensation. Similar situation occurred with data by Yun et al.[22] and Tan et al.[23] in various pore sizes of MCM-41, except in the largest pore with 8-nm diameter in the latter work. Capillary condensation of ethane in SBA-15 of three different pore size at temperatures ranging from 263 K up to PCP region has also been measured with isochoric cooling method utilizing a high-pressure micro-differential scanning calorimeter (micro-DSC).[14] However, the measurements did not go to lower temperatures due to the limitation of the micro-DSC setup.

In this work, we managed to set up the following steps toward the objective: (1) to measure the capillary condensation of ethane in MCM-41 under conditions ranging from 1.1 bar up to PCP region with isochoric cooling procedure utilizing BT 2.15 DSC; (2) to determine PCP from the capillary condensation data using the three-line method, which is further verified by measurements adopting two isochoric cooling paths close to PCP, i.e., above and below PCP; (3) to perform a gradual phase transition of ethane in MCM-41 using multistep paths starting from a point in the vapor-like region for confined ethane, then proceeding around PCP through the supercritical region, and eventually proceeding back to another point in the vapor-like region. The last objective is not only to confirm the gradual phase transition of a confined fluid, but also to establish a procedure that can be used for our future work on confined fluid mixtures for obtaining an additional proof of no phase coexistence investigated earlier.[11]

2. Materials and apparatus

The MCM-41 mesoporous silica used in this work is the same as that in our previous work,[9] which is purchased from Advanced Chemicals Supplier. The main properties are shown below in

Table 1 for convenience. Ethane gas was purchased from Airgas with a purity of 99.99%.

Two experimental setups used in this work are the same as those in our previous works.[9,16] The first setup with BT 2.15 system, which has been shown to be capable of accurately measuring the phase transition of methane, is used in this work to measure the capillary-condensation curve and PCP.[9] The BT 2.15 system mainly consists of a BT 2.15 DSC purchased from SETARAM Inc. operating in a temperature range of −196 to 200 °C with a pressure limit of 600 bar, a high-sensitivity digital pressure transducer manufactured by MENSOR with a measuring range of 0−400 bar with an accuracy of 0.01% over full span, and a syringe pump of model 500D from TELEDYNE ISCO with a cylinder capacity of 507 mL, a flow rate range of 0.001 to 204 mL/min, and a pressure range of 0.7 to 258.6 bar. Unlike the measurements using the micro-DSC system, the measurements using the BT 2.15 system is facilitated by introducing a volume buffer with a capacity of 507 mL to stabilize the pressure, which is provided by the syringe pump primarily used for adjusting the initial pressure to a desired value.[9] Small pressure fluctuations in the 3.6 mL test cell during the cooling process are damped by a much bigger volume of the buffer.

The second setup with micro-DSC system is used solely for the verification of PCP by taking two cooling paths bracketing the PCP based on the ability of the micro-DSC system to achieve a more stable heat-flow baseline at the vicinity of PCP compared to the BT 2.15 system, and thus facilitate the observation of a small heat-flow peak during capillary condensation. Baselines are the trend lines of the heat flow signals if there is no thermal event, shown as the black long dashed lines along the heat flow in the thermograms. The micro-DSC system is similar to the BT 2.15 system except that the key equipment is the micro-DSC VII purchased from SETARAM Inc., which can operate with a pressure limit of 400 bar and a temperature range of −45 to 120 °C. More details can be referred to our previous work.[16]

Table 1. Properties of the adsorbents from nitrogen adsorption isotherms at 77 K.[9§]

Sample	S_{BET}, m^2/g	V_{total}, cm^3/g	D_{BJH}, nm	D_{NLDFT}, nm
MCM-41	980.7	0.762	3.1	3.5

[§]S_{BET}, multipoint BET surface area; V_{total}, total pore volume; D_{BJH}, modal diameter of pores obtained from the BJH method desorption branch; D_{NLDFT}, modal diameter of pores obtained from the NLDFT method.

3. Experiments

3.1. Capillary condensation and PCP

The capillary condensation is measured using the following procedure. A specific amount of mesoporous silica is weighed and introduced into the test vessel. The test vessel is then introduced into the DSC. The system is evacuated to remove any remaining gas (e.g., air) inside the mesoporous silica, test vessel, tubes, and syringe pump. The gas of interest is then injected to the system and adjusted to a desired value with the syringe pump. An isochoric cooling process starts from a specified temperature and pressure in the vapor region and proceeds at a constant cooling rate of 0.05 °C/min. Through the whole cooling process, the temperature and heat flow are

recorded by the DSC, while the pressure is recorded synchronously by the pressure transducer. The same procedure is repeated for other start points at lower pressures and temperatures to produce the entire capillary-condensation curve.

The PCP is determined using the three-line approach developed in our previous work.[14] We plot the inverse of temperature and natural log of pressure at capillary condensation against the released heat. The released heat of capillary condensation is determined from the area of the small capillary-condensation peak on the thermogram. For a certain amount of nanoporous medium, this plot is linear so that three lines used in the approach represent the measurements using three different amounts of nanoporous medium. The intercept at the vertical axis, which is determined such that the linear regressions of the three lines result in the largest correlation coefficient R^2, is the point at which no heat is released, thus gives the temperature and pressure of the PCP.

3.2. Gradual phase transition

The gradual phase transition of confined ethane is performed with a two-step path starting from a point at the vapor-like region and proceeding around PCP into the liquid-like region. To verify the existence of liquid-like phase in the pores, a third step is performed to reach the vapor-like region by crossing the capillary-condensation curve. The multi-step path is shown in Figure 8 in a later section. Specifically, the whole path consists of the following steps: (1) an isothermal compression process (i.e., process AB in Figure 8): ethane in MCM-41 at 4.9 bar and 298.15 K (a specific point in the vapor-like region) is compressed to 18.7 bar and 298.15 K (supercritical region for ethane confined in MCM-41) using a syringe pump with a constant compression rate of 10 mL/min, during which the volume of the pump cylinder is reduced from 507 mL (i.e., capacity of the pump cylinder) to 100 mL; (2) an isochoric cooling process (process BC): by using the end point of step (1) as the initial point, ethane is then cooled to 17.2 bar and 266.15 K (a point at the liquid-like region) with a constant scanning rate of 0.05 K/min, as adopted in our previous works;[9,16] and (3) a polytropic process in which the fluid expansion is accompanied by cooling (process CF): the ethane is depressurized with a constant expansion rate of 0.85 mL/min utilizing the syringe pump while simultaneously being cooled with a constant scanning rate of 0.04 K/min. The depressurization and cooling rates are designed as such to make the path intersect the capillary condensation curve at a point far enough from PCP and to ensure the system inside the sample cell, at least when the phase transition occurs, can approximate equilibrium and thereby a stable baseline can be achieved. A reduced scanning rate from 0.05 K/min to 0.04 K/min is also to make the EF path distinguishable from the capillary-condensation curve in a PT diagram.

4. Results and discussion

4.1. Isochoric measurement of capillary condensation of ethane confined in MCM-41

A typical thermogram in Figure 1 shows a small distinct heat flow peak during capillary condensation followed by a big peak for bulk condensation during a single isochoric cooling procedure, as found before.[9] The capability of measuring the bulk condensation not only ensures

the accurate measurement of capillary condensation by validating against literature value of bulk condensation in NIST,[24] but also makes it possible to determine the uncertainty of the capillary condensation. During the whole measurement, the pressure drops gradually before the occurrence of bulk condensation, after which the pressure starts to drop significantly. Unlike a small pressure drop/rise observed in the thermograms at capillary condensation/evaporation using the micro-DSC system in our previous works,[10,15] the measurements of capillary condensation in this study using the BT 2.15 system do not show similar pressure drops due to the "damping effect" introduced by the volume buffer in the syringe pump. In other words, the small pressure drops, supposedly occur in the 3.6 mL test cell during the capillary condensation, are damped by the buffer.

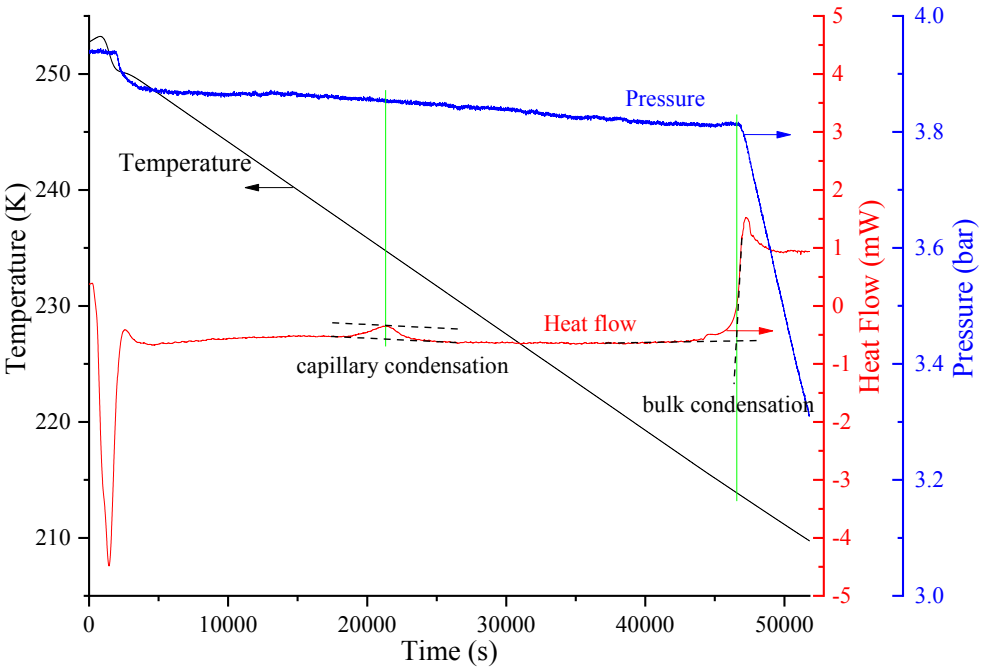

Figure 1. Typical thermogram of measurement of capillary condensation of ethane confined in MCM-41 of 3.5 nm.

The condition for capillary and bulk condensation can therefore be determined respectively from the thermogram. The full details of the procedure for determination of condensation and uncertainty of the measurements can be referred to our previous work.[9] The capillary condensation data and uncertainty analysis in this work are given in the Electronic Supplementary Information.

The P-T diagram in Figure 2 shows that the capillary-condensation curve for ethane in MCM-41 is below the bulk vapor curve, as expected. The measured bulk condensation agrees well with the literature data from NIST,[24] which confirms the accuracy of the measurements for capillary condensation. For comparison, the capillary condensation of ethane confined in MCM-41 derived from isotherms in the literature is included in Figure 2. The capillary condensation from He and Seaton [21] is at higher temperatures isobarically compared to our measurement due to smaller pore size, while that from Yun et al.[22] happens to fall on the capillary-condensation curve measured by us despite their larger sample size. It should be noted that their measurement is close

to PCP, which may introduce significant inaccuracy due to the gradual slope on the isotherms. As expected, the capillary-condensation points from Tan et al.[23] lie at lower temperatures compared to our measurement due to larger pore size.

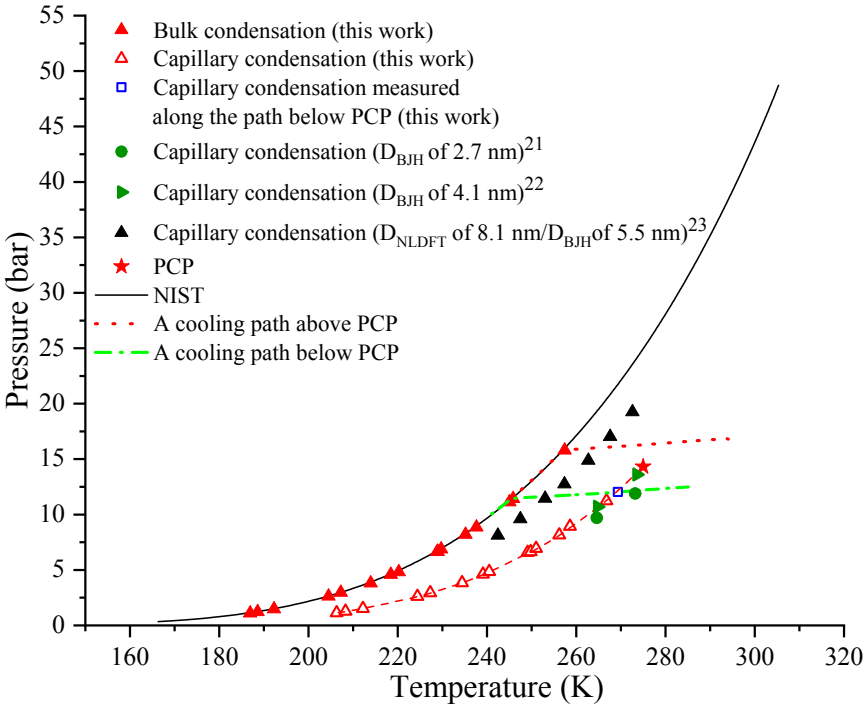

Figure 2. P-T diagram of the capillary condensation of ethane confined in MCM-41 of 3.5 nm. The dashed curve is just a guide to the eye.

4.2. Criticality of ethane in MCM-41

By using the three-line approach,[14] the PCP is determined for ethane in MCM-41. Figure 3 shows excellent linearity for reciprocal of absolute temperature and natural logarithm of pressure versus total heat during capillary condensation, which confirms the validity of the approach and measurements. The results are shown below in Table 2.

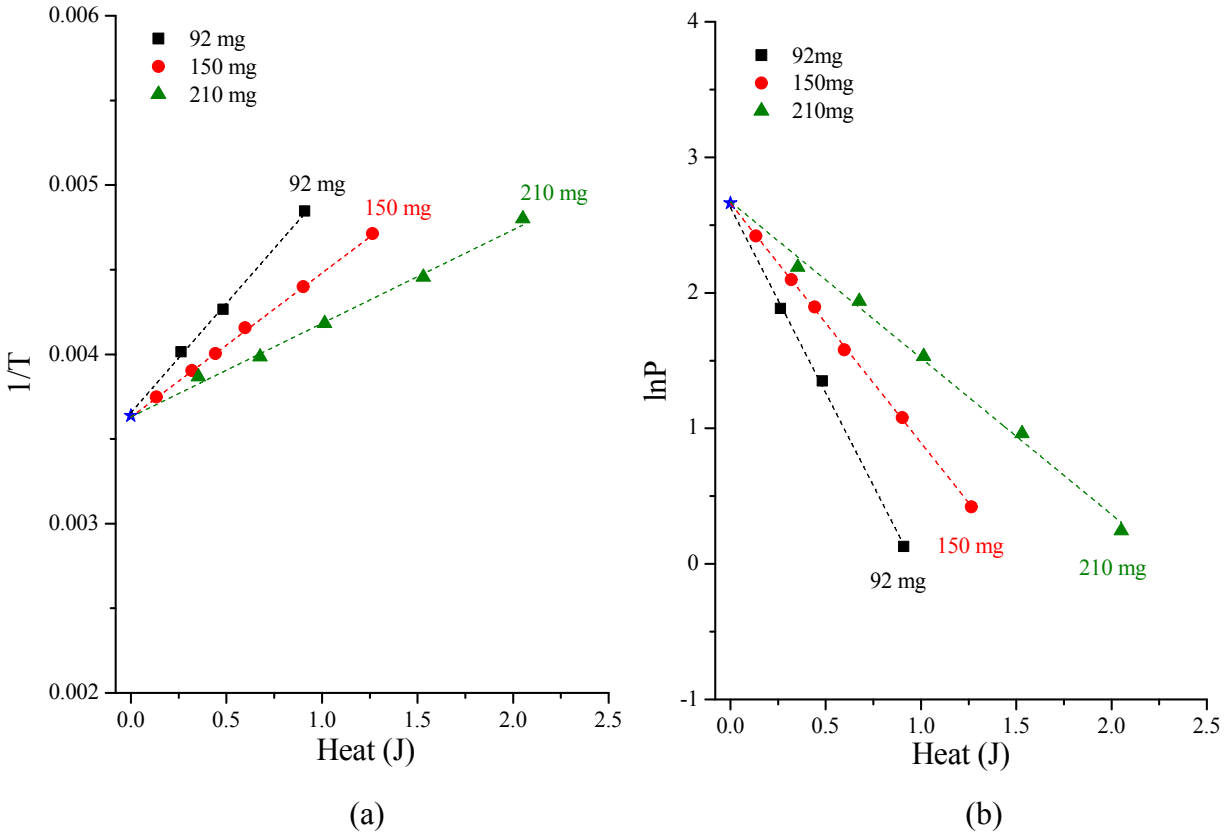

Figure 3. Three-line approach for determining (a) pore critical temperature and (b) pore critical pressure for ethane in MCM-41.

Table 2. Bulk critical point and PCP for ethane in MCM-41.

Bulk critical point from NIST		Nanopore	Pore critical point	
Temperature (K)	Pressure (bar)		Temperature (K)	Pressure (bar)
305.322	48.722	MCM-41 (3.5 nm)	$275.0\,^{+0.8}_{-1.3}$	$14.3\,^{+0.4}_{-0.4}$

It is widely recognized that the capillary condensation only happens below PCP. In other words, there should be no detection of capillary condensation peak with an isochoric cooling path above PCP, whereas a small peak should appear below PCP. Thus, the PCP can be verified by conducting two experiments along two isochoric cooling paths close to PCP using our micro-DSC system,[14] the thermograms of which are shown in Figures 4 and 5. The thermogram in Figure 4 shows the measurement with the cooling path above PCP. The heat flow is stable and no distinct small peak is observed before bulk condensation happens, i.e., before the heat flow rises sharply. The pressure drops gradually with temperature until a significant drop is observed when bulk condensation happens.

By contrast, the thermogram in Figure 5 shows a small heat flow peak, which corresponds to the capillary condensation. A small pressure drop was also detected during the capillary condensation, whereas such drop is absent in the thermogram (Figure 1) by the BT 2.15 DSC system due to the "damping effect" mentioned earlier.

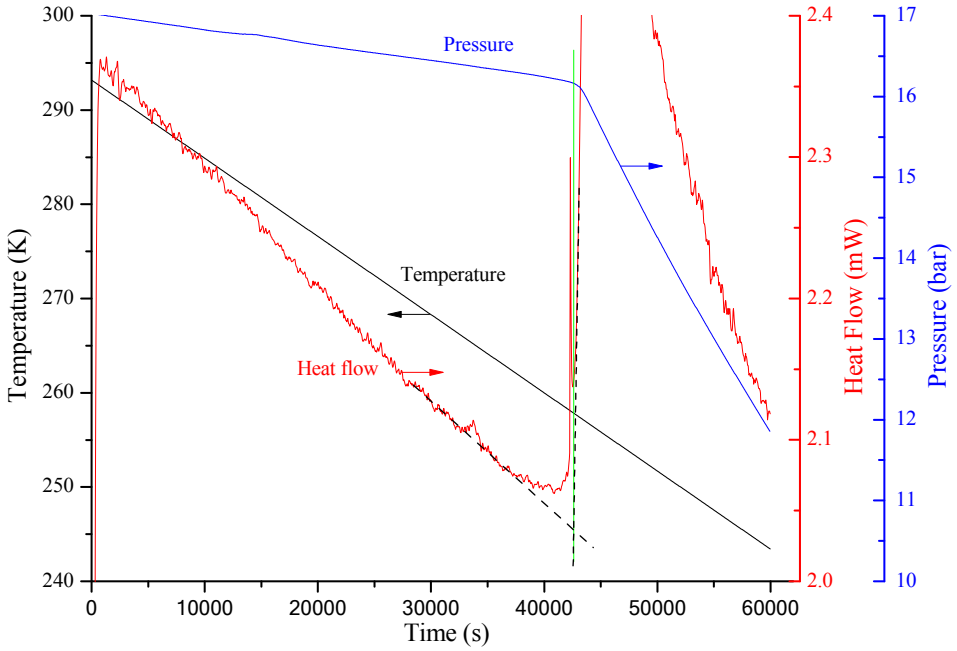

Figure 4. Thermogram of measurement of capillary condensation of ethane confined in MCM-41 along a path above PCP using micro-DSC.

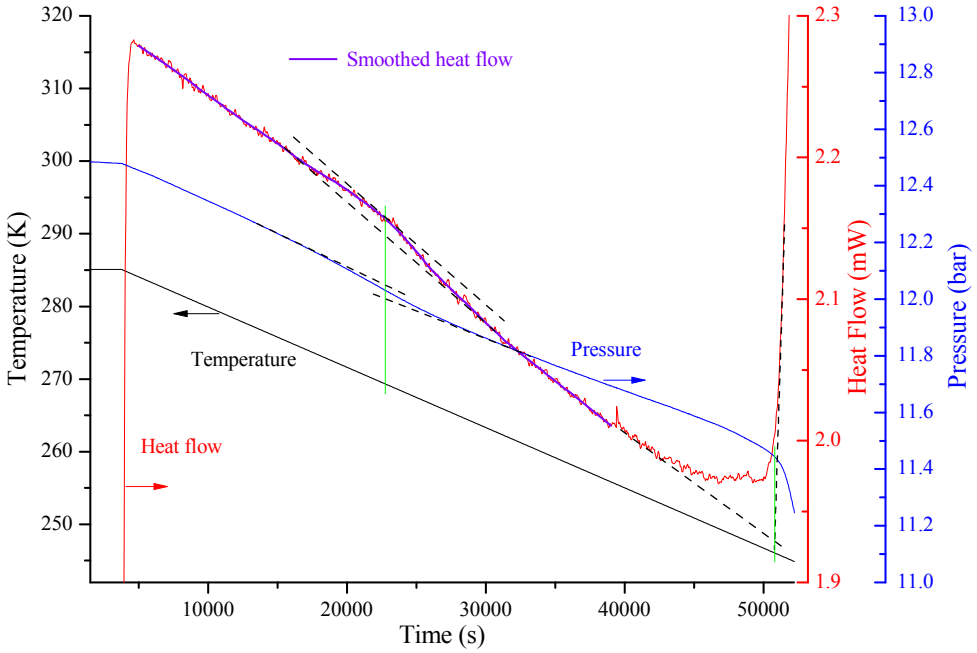

Figure 5. Thermogram of measurement of capillary condensation of ethane confined in MCM-41 along a path below PCP using micro-DSC.

As shown in Figure 2, the bulk condensation measurement is consistent with the literature value from NIST, which confirms the accurate measurement of capillary condensation by the micro-DSC. In addition, the measured condition falls on the same capillary-condensation curve measured by our BT 2.15 system. This also shows that the measurements of the same fluid using two different instruments are consistent to each other, and thus equally effective. These observations also confirm that the PCP determined by the three-line approach is accurate.

In addition, we plot a P-T diagram that also includes our previous measurements for capillary condensation and PCP of methane[9] and ethane[14] in SBA-15 and MCM-41, as shown in Figure 6. The data of ethane confined in MCM-41 of 3.5 nm are those newly measured in this work while others are from our previous works. The trend is found to be consistent, as the data in 3.5 nm pores for each fluid have the lowest condensation pressures and PCP due to the smallest pore size. However, an interesting behavior is found from cross comparison between fluids and pore types. It is observed that the trend of pore critical pressure (P_{Cp}) of methane and ethane confined in SBA-15 with similar pore size is consistent with that of critical pressures for their bulk counterparts. It is noticeable that the P_{Cp} of ethane in SBA-15 of 6.1 nm is even higher than that of methane in SBA-15 of 7.0 nm, suggesting that P_{Cp} of ethane in SBA-15 of 7.0 nm will also be higher than that of methane in this sample. In contrast, a reverse trend of P_{Cp} is observed for these fluids confined in MCM-41 with similar pore size. This may be due to stronger confinement effect for larger molecules in MCM-41 and thereby larger shift of PCP from bulk critical point compared to that in SBA-15. The pore structure of cylindrical mesopores interconnected with micropores in SBA-15 may make the confinement effects for larger molecules in SBA-15 weaker than those in MCM-41, where no micropores exists. For the record, this interesting behavior is also observed if we compare the current data for ethane with those of even larger molecules of CO_2 in SBA-15 and MCM-41.[14,25]

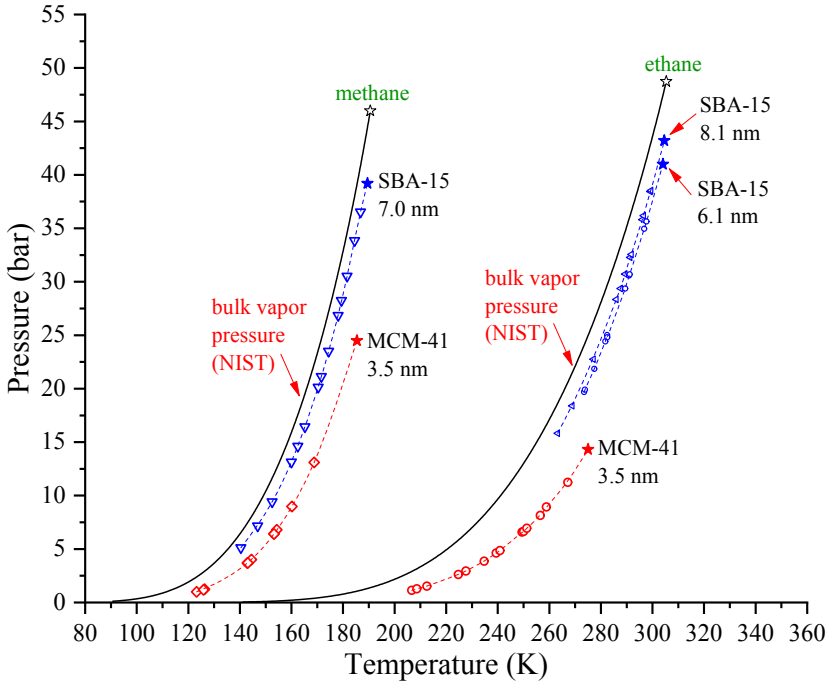

Figure 6. PCP comparison for methane and ethane in SBA-15 and MCM-41. Stars denote bulk and pore critical points. Dashed curves are just a guide to the eye.

Figure 7 shows the PCP shift of different fluids (carbon dioxide, ethane, and methane) confined in SBA-15 and MCM-41 from our current and previous experiments. The PCP shifts of fluids confined in MCM-41 do not closely follow the correlations developed for fluids in SBA-15 in our previous work.[14] To develop similar correlations for fluids in MCM-41, more experimental data are needed. Consistent with the interesting behavior discussed above, the PCP shift, which suggests the confinement effect, of ethane is larger than that of methane in MCM-41 of 3.5 nm, whereas the PCP shift of ethane in SBA-15 of pore size between 6.1 nm and 8.1 nm[14] is comparable to that of methane in SBA-15 of 7.1 nm.[9]

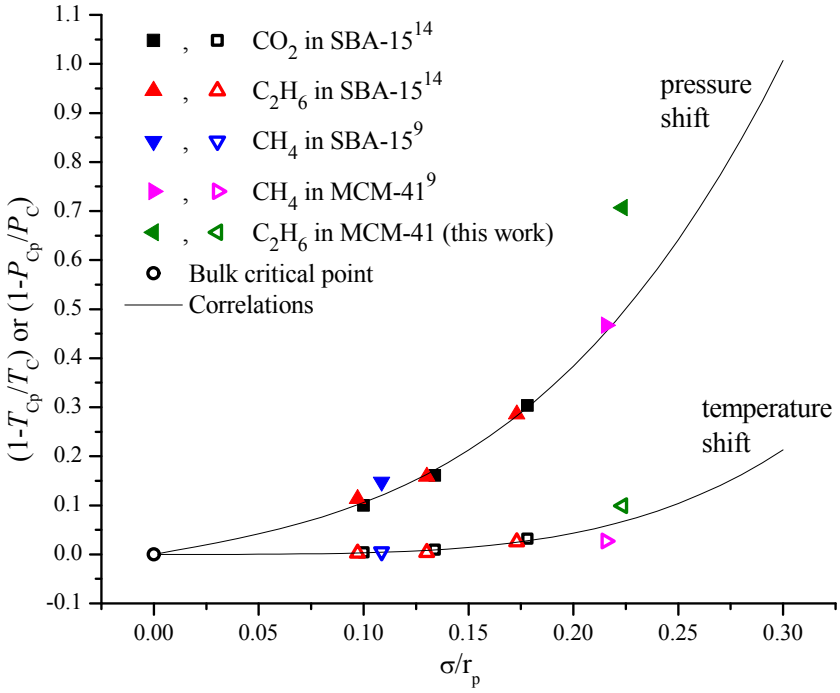

Figure 7. Behavior of the PCP-shift with respect to the ratio of Lennard-Jones molecular diameter (σ) to pore radius (r_p). The values of σ are 0.407 nm (CO_2), 0.3954 nm (C_2H_6), and 0.3817 nm (CH_4).[26] The correlations are referred to our previous work.[14]

4.3. Gradual phase transition of ethane in MCM-41

The P-T diagram in Figure 8 shows a path proceeding around PCP to perform the gradual phase transition of ethane confined in MCM-41 though the supercritical region. As observed, the gap between capillary-condensation curve and the bulk vapor curve is large, especially for the region close to PCP, which makes it possible for the CF process to cross the capillary-condensation curve at a point far from PCP by making the end point C of BC process as closely as possible to the bulk vapor curve. This ensures the heat flow peak for capillary evaporation during CF process is large enough to be observed, as shown in Figure 9.

The corresponding thermogram in Figure 9 shows that the heat flow is stable for the BC step as expected with no capillary condensation above PCP. By contrast, it is observed a distinct endothermic heat flow peak in the CF process, which is a first-order phase transition, i.e., capillary evaporation. With a constant expansion rate of 0.85 mL/min, at the early stage of this step, the pressure drops at a much higher rate before point D due to the relatively small volume of the pump cylinder and thereby an unstable heat flow line is observed. However, the heat flow gradually reaches a plateau while approaching point D and thereby a stable baseline is achieved even though the pressure still drops nonlinearly, which facilitates observation of a clear capillary evaporation peak at point E. This indicates that a sufficiently small expansion rate (e.g., 0.85 mL/min) and thereby small depressurization rate for DF process due to a large buffer can still produce a stable baseline.

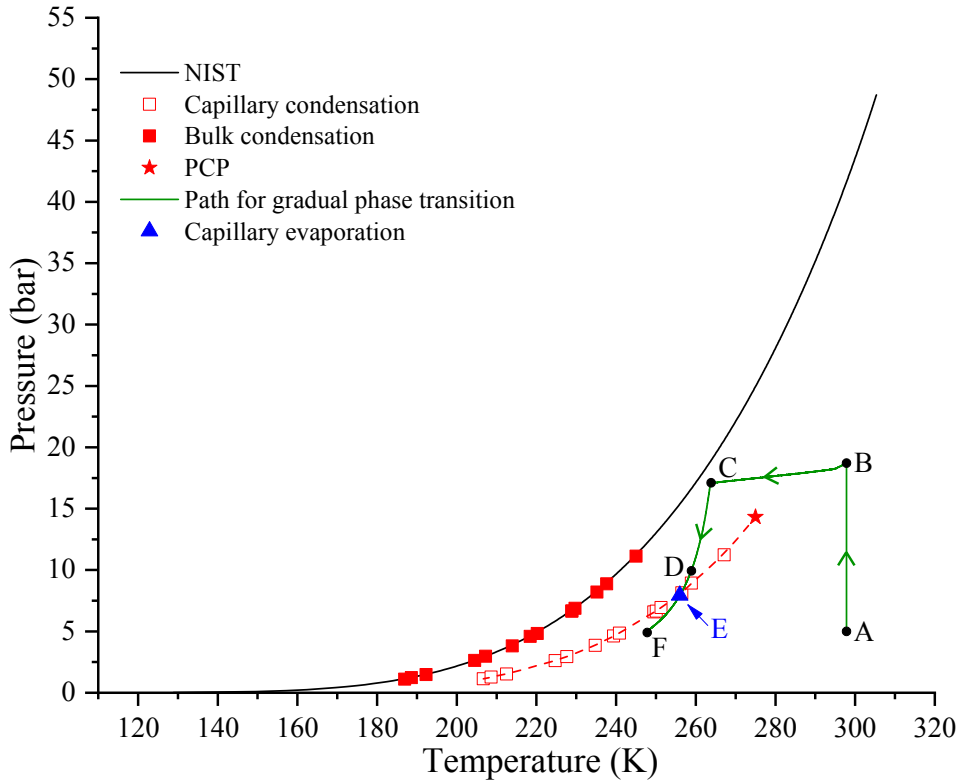

Figure 8. P-T diagram for gradual phase transition of ethane in MCM-41.

Whereas a small pressure increase/decrease during capillary evaporation/condensation is observed in our previous work,[10] similar pressure change is not observable in this measurement. The reason is that, in addition to the damping by the volume buffer discussed earlier, the volume of the fluid in the system is also increasing during the CF process as the pressure drops. Compared to the earlier stage, the volume of the system is much bigger when capillary evaporation occurs at the later stage.

The condition of capillary evaporation is also plotted in Figure 8 as point E, which shows that it falls on the capillary-condensation curve measured with the isochoric method, which further

confirms the consistency and validity of the measurements. In addition, the observed capillary evaporation peak verifies that the confined fluid at points C and D is in the liquid-like phase and that at point F in the vapor-like phase. Therefore, a gradual phase transition does occur from point A to point C.

It is worth noting that the sudden drop of the heat flow right after point C is caused by the inertia of the piston of the syringe pump, i.e., when the pump unexpectedly depressurizes with an expansion rate of 10 mL/min upon initiating the CF process. However, this does not affect our measurement since the heat flow recovers to normal level shortly and the expected capillary evaporation at point E is far from this point, and thereby a stable baseline can still be obtained. A small downward heat flow peak also appears before point D as the linear cooling rate is disturbed due to the refilling of liquid nitrogen, but with no effects on the measurement accuracies in any ways.

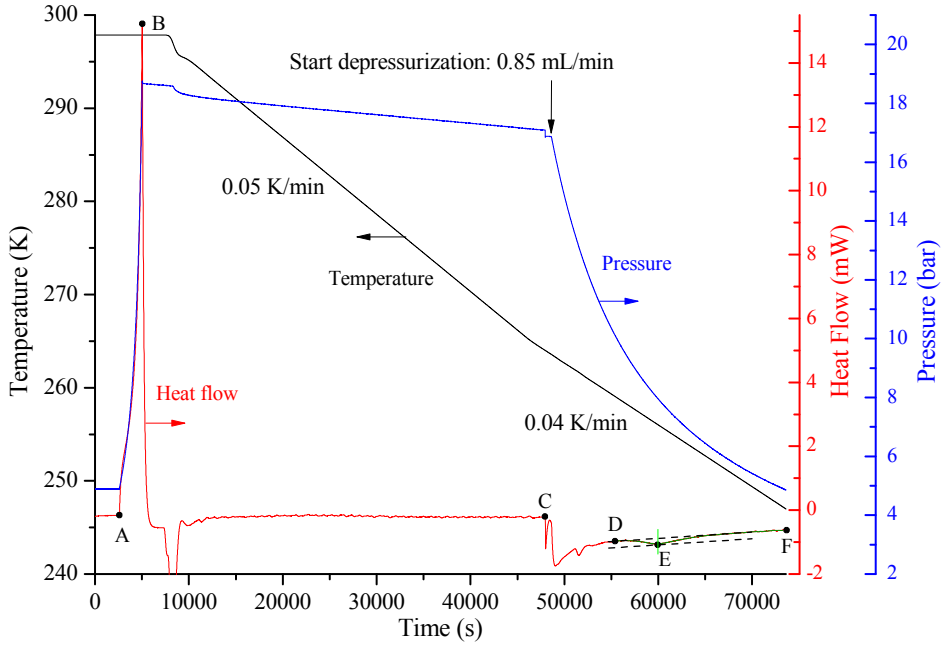

Figure 9. Thermogram for experiment of gradual phase transition of ethane in MCM-41.

5. Conclusion

The capillary condensation of ethane confined in MCM-41 has been measured under conditions ranging from 206 K and 1.1 bar up to PCP region through an isochoric cooling procedure using BT 2.15 DSC. The agreement of the measured bulk condensation with literature confirms the accuracy of the measurements for capillary condensation.

The PCP of ethane in MCM-41 has been determined using the three-line method. As found before, the plot of reciprocal of absolute temperature and natural logarithm of pressure versus total heat shows good linearity. In addition, another interesting observation we make is that the trend of P_{Cp} of methane, carbon dioxide, and ethane confined in SBA-15 with similar pore size is consistent

with that of critical pressures for their bulk counterparts, whereas a reverse trend of P_{Cp} is observed for these fluids confined in MCM-41 with similar pore size. In addition, the PCP shift of ethane confined in MCM-41 is larger than that of methane confined in the same sample, whereas the PCP shift of ethane confined in SBA-15 is similar to that of methane confined in SBA-15 with comparable pore size. The capillary condensation data and PCP determined in this work can serve as a benchmark useful for development and validation of models and simulation results.

The gradual phase transition of ethane in MCM-41 has been demonstrated by a path consisting of three steps, i.e., isothermal compression, isochoric cooling, and a polytropic process. The gradual phase transition from a vapor-like phase to a liquid-like phase without crossing the capillary-condensation curve is verified by the capillary evaporation in the polytropic step. This also experimentally confirms that there exists a supercritical region for fluids under nanoconfinement similar to that for bulk fluids. The phase transition of fluids under nanoconfinement can occur through both first-order and gradual phase transitions. The established procedure can be used to investigate additional proof of no phase coexistence for nanoconfined fluid mixtures in our future work.

Conflicts of interest

There are no conflicts to declare.

Electronic Supplementary Information

The Electronic Supplementary Information contains experimental data of capillary condensation for determining T_{Cp} and P_{Cp}, and the uncertainties of the experimental data.

Acknowledgments

This material is based upon work supported by the U.S. Department of Energy, Office of Science, Office of Basic Energy Sciences under Award Number DE-SC0021318.

References

1. Albayati, T. M. N.; Wilkinson, S. E.; Garforth, A. A.; Doyle, A. M. Heterogeneous alkane reactions over nanoporous catalysts. Transport in Porous Media **2014**, 104, 315−333.
2. Wang, Z.; Knebel, A.; Grosjean, S.; Wagner, D.; Bräse, S.; Wöll, C.; Caro, J.; Heinke, L. Tunable molecular separation by nanoporous membranes. Nature Communications **2016**, **7**, 13872.
3. Furukawa, H.; Yaghi, O. M. Storage of hydrogen, methane, and carbon dioxide in highly porous covalent organic frameworks for clean energy applications. The Journal of the American Chemical Society **2009**, 131, 8875−83.
4. Charlet, L.; Alt-Epping, P.; Wersin, P.; Gilbert, B. Diffusive transport and reaction in clay rocks: A storage (nuclear waste, CO_2, H_2), energy (shale gas) and water quality issue. Advances in Water Resources **2017**, 106, 39−59.

5. He, L.; Mei, H.; Hu, X.; Dejam, M.; Kou, Z.; Zhang, M. Advanced flowing material balance to determine original gas in place of shale gas considering adsorption hysteresis. SPE Reservoir Evaluation and Engineering **2019**, 22, 1282−1292.

6. Morishige, K.; Ito, Masataka. Capillary condensation of nitrogen in MCM-41 and SBA-15. The Journal of Chemical Physics **2002**, 117, 8036.

7. Morishige, K.; Nakamura, Y. Nature of adsorption and desorption branches in cylindrical pores. Langmuir **2004**, 20, 4503−4506.

8. Bao, B.; Zandavi, S. H.; Li, H.; Zhong, J.; Jatukaran, A.; Mostowfi, F.; Sinton, D. Bubble nucleation and growth in nanochannels, Physical Chemistry Chemical Physics **2017**, 19, 8223−8229.

9. Yang, H.; Jayaatmaja, K.; Dejam, M.; Tan, S. P.; Adidharma, H. Phase transition and criticality of methane confined in nanopores. Langmuir **2022**, 38, 2046−2054.

10. Qiu, X.; Yang, H.; Dejam, M.; Tan, S. P.; Adidharma, H. Experiments on the capillary condensation/evaporation hysteresis of pure fluids and binary mixtures in cylindrical nanopores. The Journal of Physical Chemistry C **2021**, 125, 5802−5815.

11. Qiu, X.; Tan, S. P.; Dejam, M.; Adidharma, H. Binary fluid mixtures confined in nanoporous media: Experimental evidence of no phase coexistence. Chemical Engineering Journal **2021**, 405, 127021.

12. Qiu, X.; Tan, S. P.; Dejam, M.; Adidharma, H. Isochoric measurement of the evaporation point of pure fluids in bulk and nanoporous media using differential scanning calorimetry, Physical Chemistry Chemical Physics **2020**, 22, 7048−7057.

13. Qiu, X.; Tan, S. P.; Dejam, M.; Adidharma, H. Experimental study on the criticality of a methane/ethane mixture confined in nanoporous media. Langmuir **2019**, 35, 11635−11642.

14. Tan, S. P.; Qiu, X.; Dejam, M.; Adidharma, H. Critical point of fluid confined in nanopores: Experimental detection and measurement, The Journal of Physical Chemistry C **2019**, 123, 9824−9830.

15. Qiu, X.; Tan, S. P.; Dejam, M.; Adidharma, H. Simple and accurate isochoric differential scanning calorimetry measurements: Phase transitions for pure fluids and mixtures in nanopores. Physical Chemistry Chemical Physics **2019**, 21, 224−231.

16. Qiu, X.; Tan, S. P.; Dejam, M.; Adidharma, H. Novel isochoric measurement of the onset of vapor–liquid phase transition using differential scanning calorimetry. Physical Chemistry Chemical Physics **2018**, 20, 26241−26248.

17. Luo, S.; Lutkenhaus, J. L.; Nasrabadi, H. Use of differential scanning calorimetry to study phase behavior of hydrocarbon mixtures in nano-scale porous media. Journal of Petroleum Science and Engineering **2018**, 163, 731−738.

18. Naumov, S.; Valiullin, R.; Monson, P. A.; Kärger, J. Probing memory effects in confined fluids via diffusion measurements. Langmuir **2008**, 24, 6429−6432.
19. Chiang, W. -S.; Fratini, E.; Baglioni, P.; Chen, J. -H.; Liu, Y. Pore size effect on methane adsorption in mesoporous silica materials studied by small-angle neutron scattering. Langmuir **2016**, 32, 8849−8857.
20. Levelt Sengers, J.M.H. In Supercritical Fluids: Their Properties and Applications in: Supercritical Fluids—Fundamentals and Applications (eds. Kiran, E. et al.) 1–29 (Kluwer Academic Publishers, Berlin, 2000).
21. He, Y.; Seaton, N. A. Experimental and computer simulation studies of the adsorption of ethane, carbon dioxide, and their binary mixtures in MCM-41. Langmuir **2003**, 19, 10132−10138.
22. Yun, J.-H.; Düren, T.; Keil, F. J.; Seaton, N. A. Adsorption of methane, ethane, and their binary mixtures on MCM-41: experimental evaluation of methods for the prediction of adsorption equilibrium. Langmuir **2002**, 18, 2693−2701.
23. Tan, S. P.; Barsotti, E.; Piri, M. Criticality of confined fluids based on the tensile strength of liquids. Industrial & Engineering Chemistry Research **2020**, 59, 10673-10688.
24. Lemmon, E. W.; McLinden, M. O.; Friend, D. G. Thermophysical Properties of Fluid Systems. In NIST Chemistry WebBook, NIST Standard Reference Database Number 69; Linstrom, P. J.; Mallard, W. G.; Eds.; National Institute of Standards and Technology (NIST): Gaithersburg, MD, **2017**. DOI: 10.18434/T4D303 (accessed Mar 2022).
25. Morishige, K.; Nakamura, Y. Nature of adsorption and desorption branches in cylindrical pores. Langmuir **2004**, 20, 4503−4506.
26. Hirschfelder, J. O.; Curtiss, C. F.; Bird, R. B. Molecular theory of gases and liquids; John Wiley & Sons, Inc.: New York, **1964**.